

Supporting Information

An Ion Mobility-Mass Spectrometry Study of Copper-Metallothionein-2A: Binding Sites and Stabilities of Cu-MT and Mixed Metal Cu-Ag and Cu-Cd Complexes

Liqi Fan and David H. Russell*
Department of Chemistry
Texas A&M University
College Station, TX 77843

*Corresponding author, email: russell@chem.tamu.edu

Table of Contents

| Figures | Page |
|--|------|
| S1. Molecule fraction of Cu-MT species versus Cu concentration in the titration experiment. | S2 |
| S2. CIU heatmap of Cu ₆ NEM ₁₁ -MT and Cu ₁₀ NEM ₅ -MT | S2 |
| S3. Zoomed-in mass spectra of 2+ and above ions from extracted 2D-MS-CID-MS experiment and 2D spectrum | S3 |
| S4. Example of zoomed-in isotope distribution of tryptic digested fragments that contain Cu ions | S4 |
| S5. CID spectrum of Cu ₁₀ NEM ₅ -MT | S4 |
| S6. Tryptic digestion spectra of Cu ₆ NEM ₁₁ -MT and Cu ₁₀ NEM ₅ -MT | S5 |
| S7. Overlapping of Cu ₆ -MT and Cu ₁ Ag ₃ -MT in mixed-metal titrations | S6 |
| S8. Titration of a Cd ₄ -MT equilibrium solution with Cu ²⁺ | S6 |
| S9. CCS distribution of multiple metalated MTs corresponding to CIU heatmaps in Figure 6. | S7 |
| S10. Variable-temperature IMS for Cu ₆ -MT and Cu ₁₀ -MT | S8 |

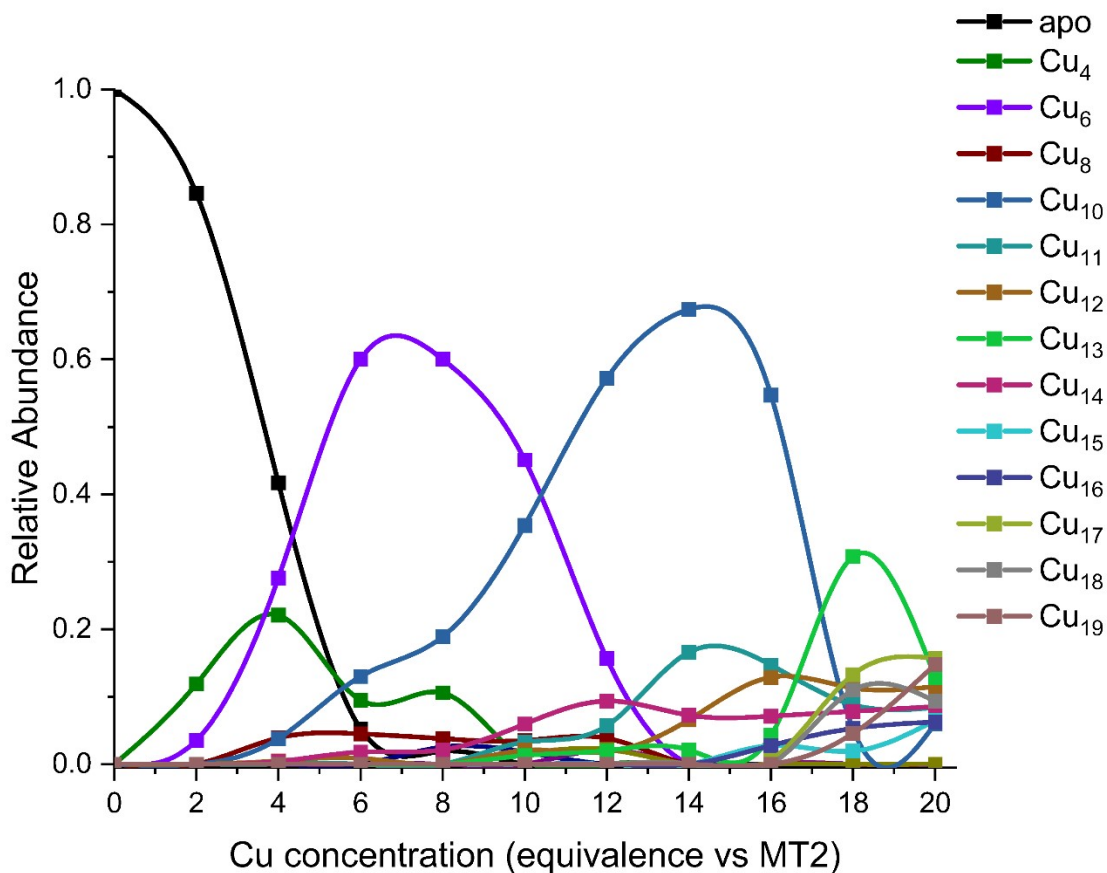


Figure S1. Molecule fraction of Cu-MT species versus Cu concentration in the titration experiment.

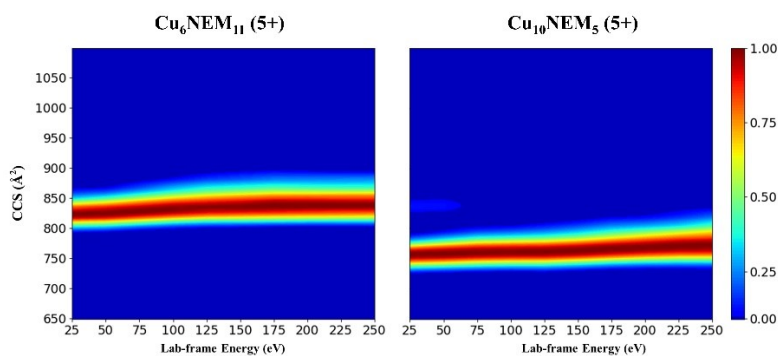


Figure S2. CIU heat map of $\text{Cu}_6\text{NEM}_{11}\text{-MT}$ and $\text{Cu}_{10}\text{NEM}_5\text{-MT}$. The addition of NEM increases the CCS of $\text{Cu}_6\text{-MT}$ significantly from ~ 750 to 850 \AA^2 (see Figure 5, main text), and the CCS of $\text{Cu}_{10}\text{NEM}_5\text{-MT}$ differs very little from that of $\text{Cu}_{10}\text{-MT}$. The CCS of both $\text{Cu}_6\text{NEM}_{11}\text{-MT}$ and $\text{Cu}_{10}\text{NEM}_5\text{-MT}$ exhibit small increases at higher collision energy that would be expected if the structures rearrange as a result of collisional heating.

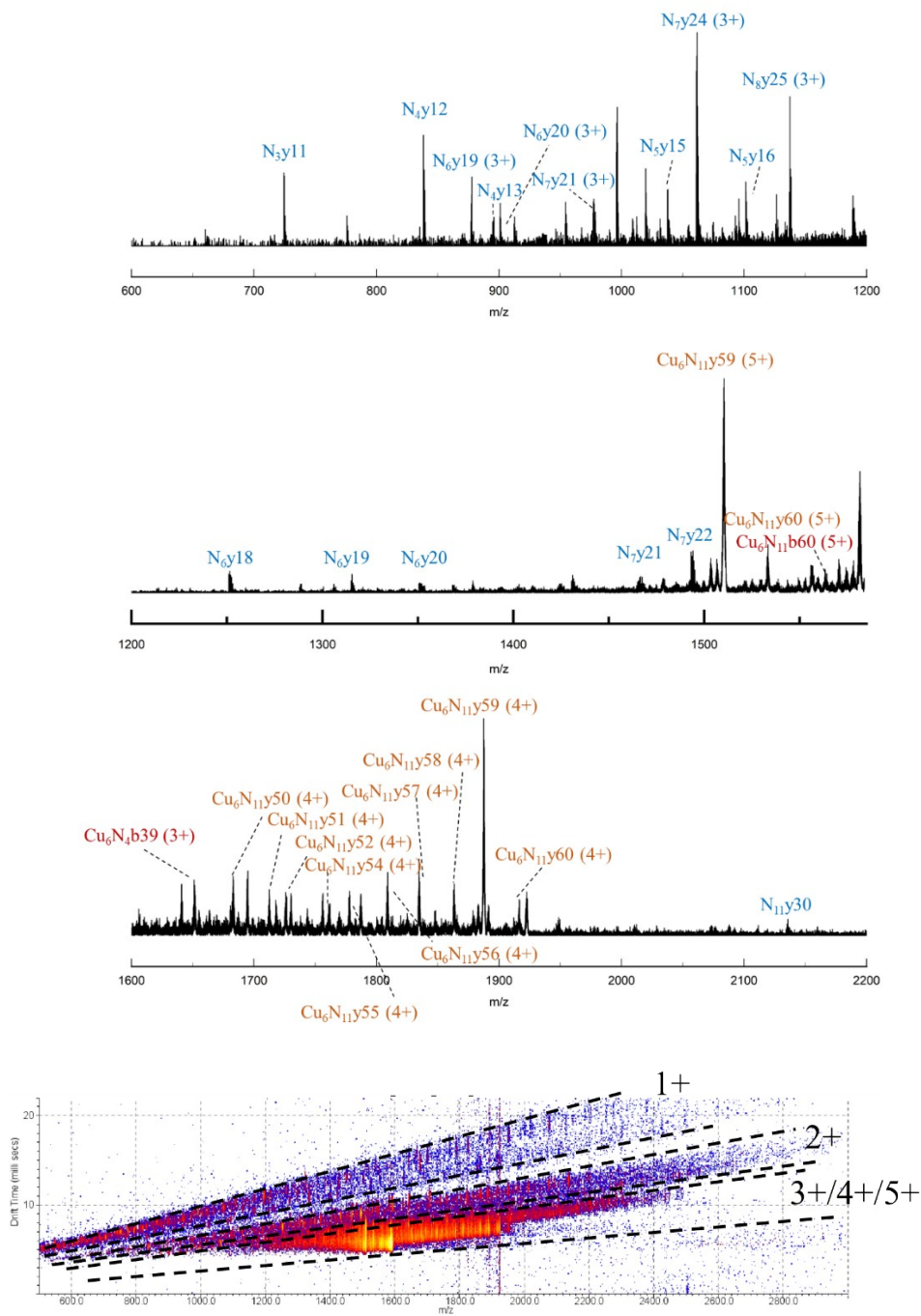


Figure S3. Mass spectra for 2⁺/3⁺/4⁺/5⁺ CID fragment ions of Cu₆NEM₁₁-MT obtained from the extracted 2D-MS-CID-MS experiment in different m/z ranges. NEM is abbreviated as N. Bottom is the plot of ion mobility arrival-time distributions versus m/z ratios obtained using 2D-IMS-CID-MS

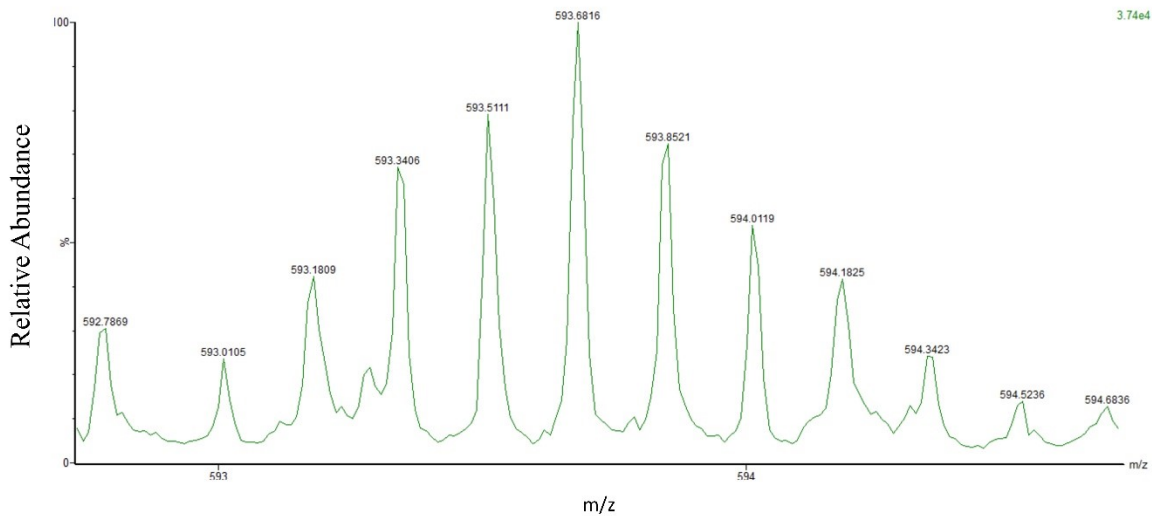


Figure S4. Expanded mass spectrum shows the isotope distribution of tryptic digested fragments that contain Cu ions. This peak is for the 6^+ Gly-Ser-1-30 fragment with 6 Cu^+ and no NEM.

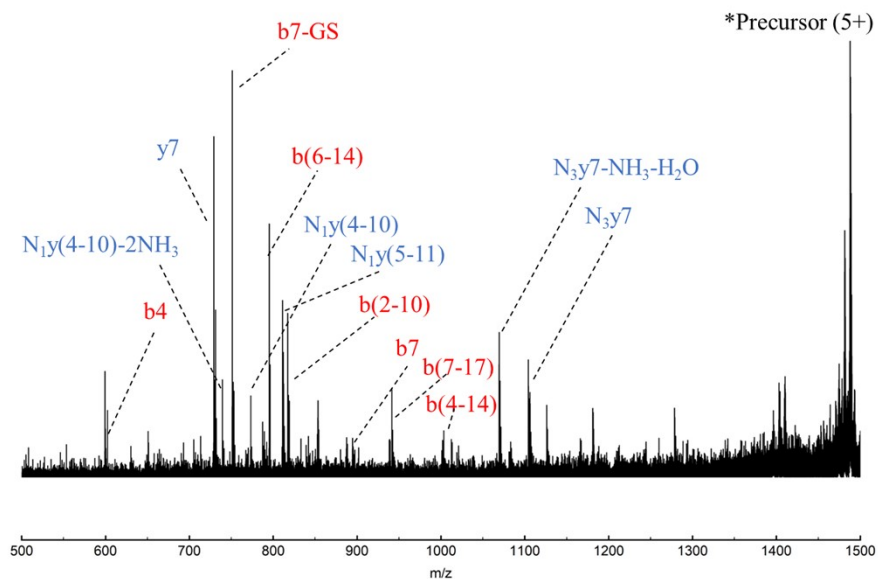
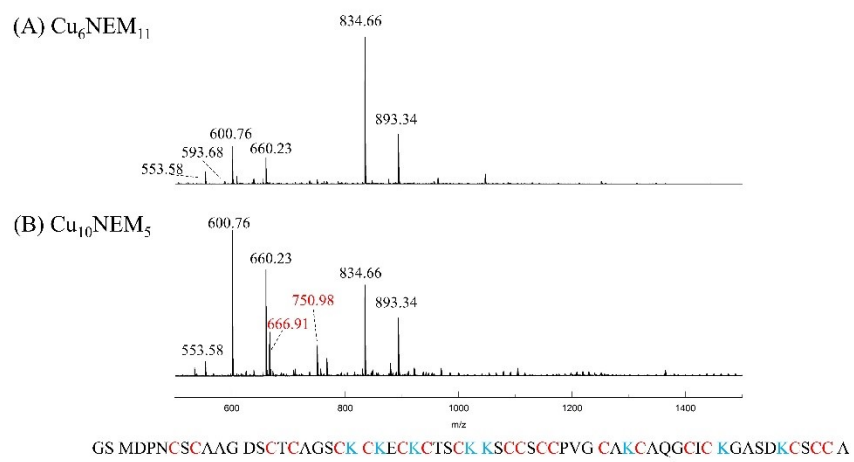


Figure S5. Top-down CID spectrum of $[\text{Cu}_{10}\text{NEM}_5\text{-MT}]^{5+}$. Annotation of internal fragments are shown in numbers, e. g. the fragments from N-terminus b2 to b10 is labelled as b(2-10).



| m/z | z | position | #Cu | #NEM | Sequence |
|--------|---|----------|-----|------|------------------------------------|
| 593.68 | 6 | GS-1-30 | 6 | 0 | GSMDPNCSCAAGDSCTCAGSCKCKECKCTISKCK |
| 893.34 | 2 | 32-43 | 0 | 5 | SCCSCPVGCAK |
| 600.76 | 2 | 44-51 | 0 | 3 | CAQGCICK |
| 834.66 | 3 | 44-61 | 0 | 6 | CAQGCICKGASDKCSCCA |
| 660.23 | 2 | 52-61 | 0 | 3 | GASDKCSCCA |
| 553.58 | 3 | 44-56 | 0 | 3 | CAQGCICKGASDK |

| m/z | z | position | #Cu | #NEM | Sequence |
|---------|---|----------|-----|------|---|
| 666.91 | 3 | 44-61 | 4 | 0 | CAQGCICKGASDKCSCCA |
| 750.98 | 3 | 44-61 | 4 | 2 | CAQGCICKGASDKCSCCA |
| 1364.36 | 4 | GS-1-43 | 6 | 5 | GSMDPNCSCAAGDSCTCAGSCKCKECKCTISKCKSCCSCPVGCAK |
| 893.34 | 2 | 32-43 | 0 | 5 | SCCSCPVGCAK |
| 600.76 | 2 | 44-51 | 0 | 3 | CAQGCICK |
| 834.66 | 3 | 44-61 | 0 | 6 | CAQGCICKGASDKCSCCA |
| 660.75 | 2 | 52-61 | 0 | 3 | GASDKCSCCA |

Figure S6. Trypsin digestion mass spectra of Cu_6 (A) and Cu_{10} -MT (B). Featured fragments containing Cu and NEM are shown in the table.

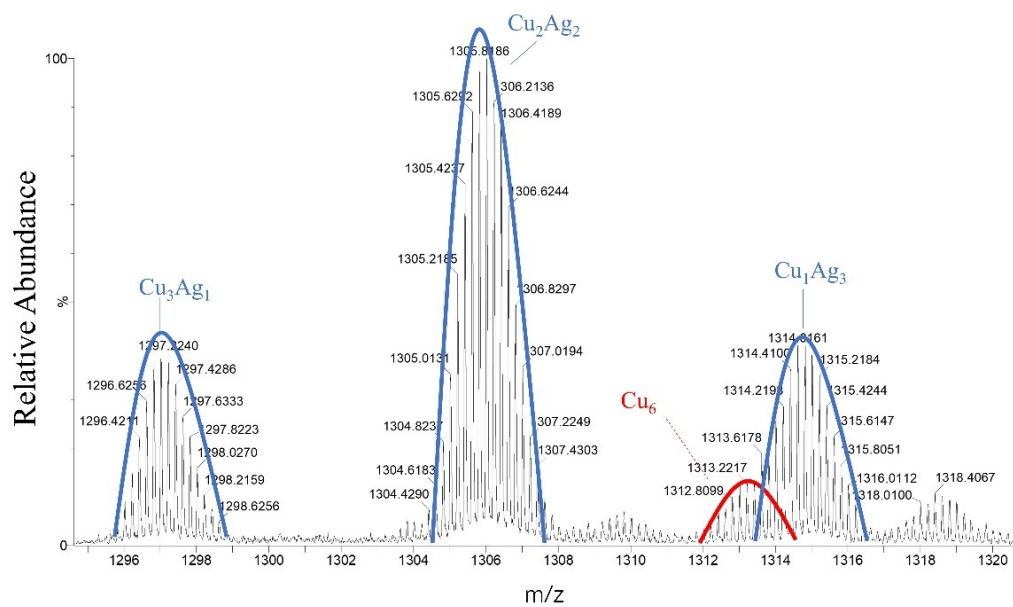


Figure S7. Mass spectrum showing the overlap of signals for $\text{Cu}_1\text{Ag}_3\text{-MT}$ and $\text{Cu}_6\text{-MT}$. Two isotope distributions are observed, and each is assigned to the products.

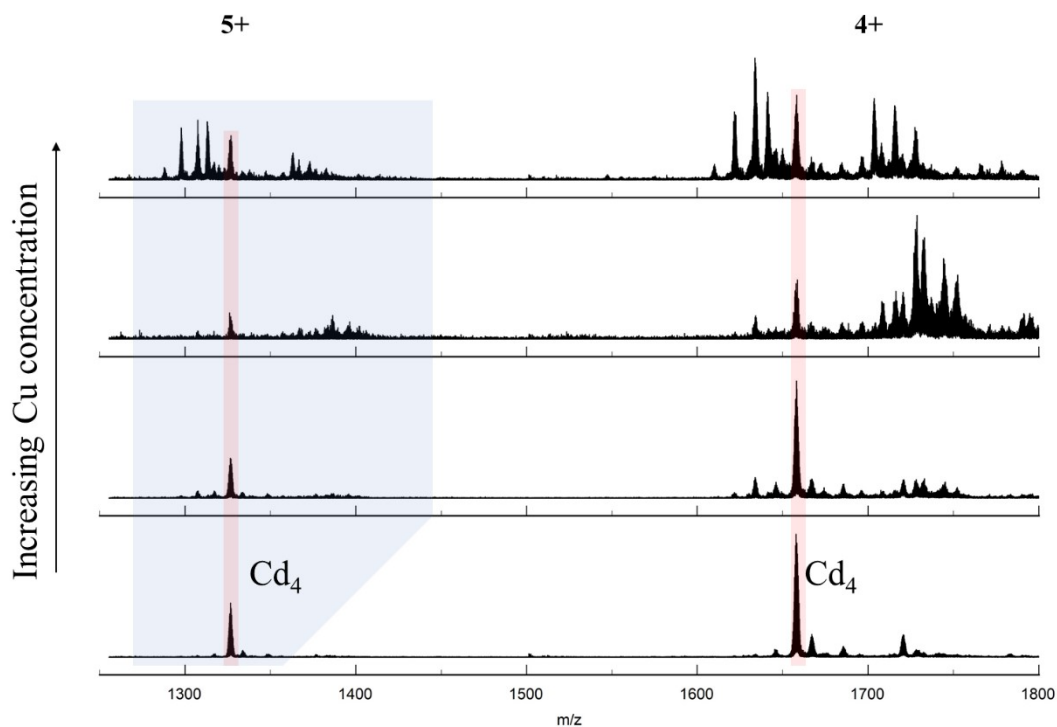


Figure S8. Mass spectra during the Cu^{1+} titration of a $\text{Cd}_4\text{-MT}$ solution. The abundances of $\text{Cd}_4\text{-MT}$ ions are retained and no new signals for Cd-Cu mixed metal complexes indicating Cd displacement by Cu^{1+} are detected. Higher order Cu/Cd-MT s products are formed as shown in Figure 4A.

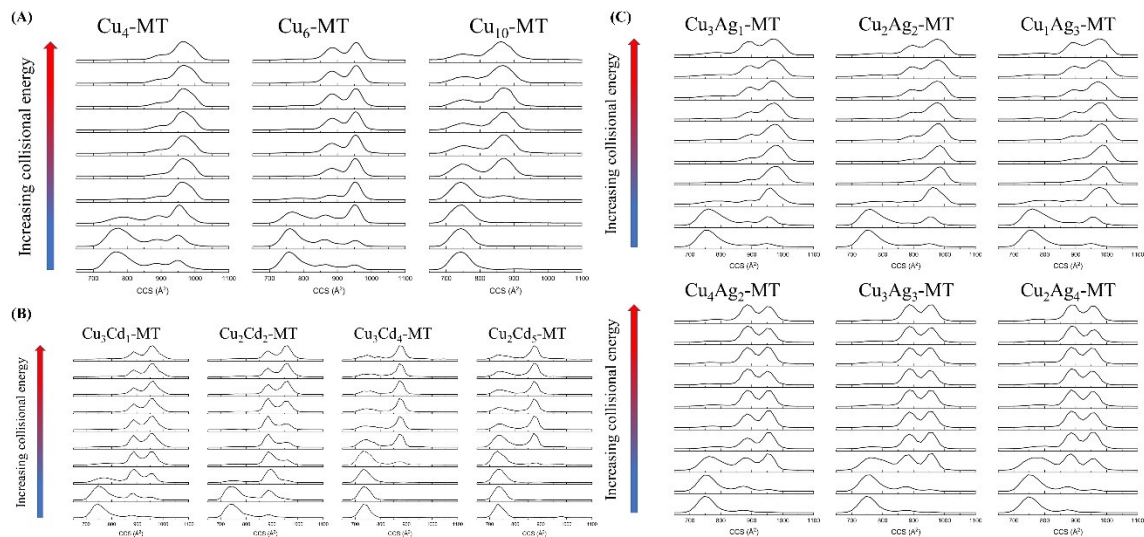


Figure S9. CCS distribution for (A) Cu₄-, Cu₆-, and Cu₁₀-MT, (B) Cu/Cd-MTs, (C) Cu/Ag-MTs corresponding to CIU profiles in **Figure 6** (in main text). The CCS distributions are directly related to the color in the CIU heatmaps, with the highest relative abundance shown in red. Lab-frame collision energies are 25 eV to 250 eV (in 25 eV increments see Experimental section).

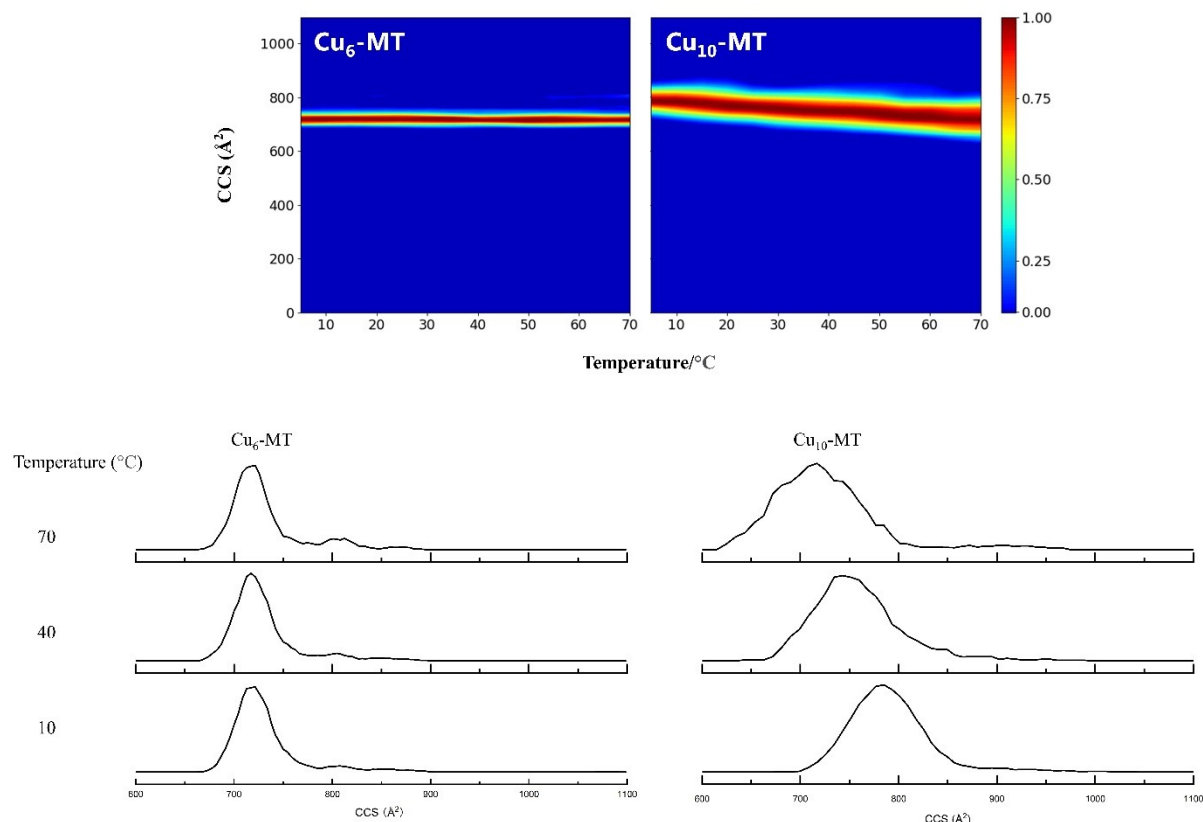


Figure S10. Temperature-induced unfolding (TIU) heatmaps of $\text{Cu}_6\text{-MT}^{5+}$ and $\text{Cu}_{10}\text{-MT}^{5+}$ complexes. In this experiment, the temperature of the solution contained in the ESI emitter is controlled by a thermoelectric chip (Peltier chip) as described previously.¹ The CCS profiles for $\text{Cu}_6\text{-MT}^{5+}$ are quite narrow and do not vary with temperature between 5 and 70 $^\circ\text{C}$, however, the CCS profiles for $\text{Cu}_{10}\text{-MT}^{5+}$ are broad and the broadness increases as temperature is increased. Moreover, the centroid in the CCS profile for $\text{Cu}_{10}\text{-MT}^{5+}$ decreases (~ 800 vs 740 \AA^2) as temperature increases. The selected CCS profiles of 10, 40 and 70 $^\circ\text{C}$ are shown under the TIU heatmaps. The changes in the width of CCS profile and the decrease in CCS are clear evidence that the conformational heterogeneity and conformational preferences of the $\text{Cu}_{10}\text{-MT}$ complex are temperature dependent. Further investigations are currently underway with a range of metal-MT complexes, *viz.* Zn, Cd and Ag to test whether this is broadly observed for metallothionein complexes.

Reference

1. J. W. McCabe, M. Shirzadeh, T. E. Walker, C.-W. Lin, B. J. Jones, V. H. Wysocki, D. P. Barondeau, D. E. Clemmer, A. Laganowsky and D. H. Russell, *Analytical Chemistry*, 2021, **93**, 6924-6931.